American Mineralogist, Volume 88, pages 1015–1019, 2003

Chemistry of grain boundaries in mantle rocks

TAKEHIKO HIRAGA,[1,*] IAN M. ANDERSON,[2] AND DAVID L. KOHLSTEDT[1]

[1]Department of Geology and Geophysics, University of Minnesota, Minneapolis, Minnesota 55455, U.S.A.
[2]Metals and Ceramics Division, Oak Ridge National Laboratory, Oak Ridge, Tennessee 37831, U.S.A.

ABSTRACT

The compositions of olivine grain boundaries have been analyzed with scanning transmission electron microscopy (STEM) via energy dispersive X-ray (EDX) spectrum profiling in three specimens: a peridotite ultramylonite, olivine phenocrysts in a basaltic rock, and synthesized compacts of olivine + diopside. Composition profiles across grain boundaries in both natural and synthetic samples exhibit a characteristic width of 5 nm and a depletion of Mg and concomitant enrichments of Ca, Al, Ti, and Cr. Chemical segregation is known to affect grain boundary processes such as grain boundary diffusion, sliding, fracture, and migration, all of which influence the rheological properties of polycrystalline aggregates. Also, because grain boundaries are enriched in trace elements, the boundaries can be important storage sites for such elements in mantle rocks. Mantle-derived melts with unusual compositions, such as those rich in Ca and/or Ti, might be explained by preferential melting of olivine grain boundaries enriched in these elements. The common chemical signatures at grain boundaries in all samples indicate that chemical segregation is an energetically favorable phenomenon and thus should occur elsewhere in Earth's mantle. Segregation of trace elements to grain boundaries may play an important role in dynamical and geochemical processes in Earth's mantle.

INTRODUCTION

In polycrystalline materials, segregation of elements to grain boundaries commonly affects the physical and mechanical properties of an aggregate with significant implications for geological processes. Grain boundaries can store significant amounts of trace elements otherwise essentially insoluble in the aggregate, consequently influencing the chemistry of rocks. Grain boundary diffusion, sliding, fracture, and migration are markedly influenced by such segregation, which thereby impacts rheological behavior. For example, Gribb and Cooper (1998) attributed the anomalously high activation energy that they observed for Coble creep of an olivine aggregate to segregation of Ca to the grain boundaries.

Grain boundaries in most mantle rocks are narrow and do not contain secondary phase material such as an amorphous film commonly observed in sintered ceramics (Hiraga et al. 2002). The concentrations of elements such as Ca, Al, and Sr at grain boundaries have been determined for some mantle rocks (e.g., Fraser et al. 1984; Suzuki 1987; Wirth 1996). However, the origin of chemical enrichment of some elements (i.e., chemical segregation) at grain boundaries in rocks is not well understood. Geological phenomena such as partial melting, metasomatism, segregation during cooling, and weathering may all lead to enhanced concentrations of impurities at grain boundaries. The question remains "does grain boundary segregation occur in Earth's mantle?"

Here, we demonstrate that a common set of elements segregates to olivine grain boundaries in both natural and synthetic olivine aggregates. The commonality of the behavior suggests that such segregation is energetically favorable and indicates that such segregation likely occurs in the Earth's mantle.

* E-mail: hirag001@umn.edu

EXPERIMENTAL PROCEDURES

STEM/EDX spectrum profiles were acquired from olivine-olivine grain boundaries using a Philips CM200FEG TEM/STEM equipped with a Schottky field emission gun (FEG), an Oxford EDX detector with atmospheric thin window and XP3 pulse processor, and an EMiSPEC (ES) Vision integrated acquisition system. The microscope was operated at an accelerating voltage of 200 kV, and the lens excitations and beam-defining apertures were chosen to achieve an incident probe of ~1.4 nm full width at half maximum (FWHM) and 1.5 nA beam current. To minimize the effects of beam damage, the STEM was set up to raster the beam parallel to the analyzed boundary in a rapid manner (~15 ms line time) so as to prevent prolonged exposure to any point on the sample. The ES Vision system was operated independently such that a single raster of the electron beam contributed to a single 250 ms per pixel of the spectrum profile. A sequence of 10 profiles was acquired from each boundary, which were then summed to yield a single, integrated profile with 2.5 s total acquisition time per pixel. Additional profiles (beyond about 10) from the same boundary exhibited beam damage, rendering ineffectual the improved statistics of more prolonged data acquisition. These methods are described in more detail elsewhere (Hiraga et al. 2002). Net counts above background were determined using the multiple linear least squares (MLLSQ) fitting procedure in Desktop Spectrum Analyzer (DTSA) (Fiori et al. 1992). This method requires the use of spectral references, which show the distribution of intensity among a family of characteristic X-ray lines for a given element, e.g., Fe*K*. For the major elements (Mg, Si, and Fe), the references were the best-fit superposition of gaussian peaks generated by applying the simplex fitting procedure within DTSA to a spectrum from the olivine matrix. For the minor and trace elements segregated to the boundary, spectral references were simulated with the spectral generation function of DTSA, using the best-fit parameters (e.g., spectral calibration and detector resolution) identified from the fit of the major elements. In the absence of spectral intensity

0003-004X/03/0007–1015$05.00

for a given element, the MLLSQ fitting procedure returns a small finite value for the intensity that can be positive or negative depending upon the random local curvature of the X-ray background; the size of these intensity fluctuations are a true measure of the noise level of the measurement. Elemental concentrations were extracted from the measurements of characteristic X-ray counts above background using the standard Cliff-Lorimer method. For this method, sensitivity factors for the major elements were determined using the matrix as a standard of composition determined by electron-probe microanalysis. The comparable sensitivity factors for the segregants were determined using a linear interpolation of the factors for the major element with atomic number. The accuracy of this interpolation is estimated to be 5–10%, which was deemed adequate given the statistical limitations of the measurement. The X-ray profiles indicated a specimen of constant thickness and showed no evidence of grain boundary grooving; for example, the O*K*, Si*K*, and Fe*K* X-ray intensity profiles were constant across the boundary. The sensitivity factors were therefore considered intrinsically absorption corrected at the specimen thickness of the data acquisition.

SAMPLES

Most olivine-bearing rocks of mantle origin have fractured (open) and/or altered (e.g., serpentinized) grain boundaries. Hence, it is difficult to determine the grain boundary structure and chemistry as they originally were deep in the Earth. We carefully selected two natural samples with clean (unaltered) and closed grain boundaries.

The first specimen is a peridotite ultramylonite from the Balmuccia peridotite in the Ivrea Zone of northwestern Italy (e.g., Shervais 1979). The Balmuccia peridotite is a mantle-derived spinel lherzolite massif primarily composed of olivine, orthopyroxene, and clinopyroxene. The rock we used is mainly made up of small (~5 μm) equidimensional grains with a well-developed foliation, as described by Jin et al. (1998). The ultramylonite adjoins pseudotachylyte veins (Obata and Karato 1995; Jin et al. 1998). Preliminary TEM observations reveal that some boundaries and intergranular cracks are filled with amorphous material. The amorphous phase is irregular in shape, suggesting that textural equilibrium was not attained. Jin et al. (1998) suggested that brittle deformation post-dated dynamic recrystallization. The equilibrium temperature T = 1300–1500 K and pressure P = 1.3–2.0 GPa for the rock have been estimated by geothermo-barometers and phase-equilibrium constraints (Shervais 1979). Many grain boundaries in the rocks are closed, unlike the boundaries in typical mantle peridotites. The superior quality of the grain boundaries likely results from the relatively small stress concentration at incipient grain boundary cracks in rocks with a fine grain size (Cooper 1990).

The second specimen is a basaltic rock with olivine phenocrysts collected from Kilauea, Hawaii. Olivine is the dominant or sole phenocryst mineral in these specimens. The gas and melt inclusions in olivine from the Kilauea Iki lava lake and scoria indicate crystallization at depths of <6 km (Harris and Anderson 1983). Two or more olivine phenocrysts are commonly in contact, forming a glomeroporphyritic texture. Individual crystals that initially grew separately, apparently come into contact during flow with the host magma (Schwindinger and Anderson 1989). Phenocrysts commonly exhibit distinct crystal faces and are in contact with other grains along such faces. Grain boundaries formed between the phenocrysts contain lens-shaped glass inclusions that were trapped during the contact. Although olivine grains in the rock may not be of mantle origin, closed and straight grain boundaries, which are rare in olivine rocks, are appropriate for our study of olivine grain boundaries.

An additional aggregate composed of olivine and diopside was prepared. A diopside aggregate synthesized from high-purity diopside glass was crushed to form a powder with a particle size of ~10 μm. This powder was then mechanically mixed with powdered dry San Carlos olivine with a similar particle size. The powder mixture was cold-pressed into a nickel capsule with a uniaxial pressure of 200 MPa and, subsequently, isostatically hot-pressed at 1473 K and 300 MPa for 5 h in a gas-medium apparatus. After hot-pressing, the aggregate contained a few pores but no amorphous phase, indicating the absence of melting. The sample was then annealed in a one-atmosphere furnace at 1373 K for 240 h with the oxygen fugacity held near the Ni-NiO buffer through controlled concentrations of CO and CO_2. All annealing processes were performed at a temperature well below the forsterite + diopside solidus (~1653 K). Finally, the sample was quenched by dropping into water. Cracks formed due to thermal shock, especially along some of the grain boundaries; however, many closed boundaries remained for TEM analysis. The grains of the synthetic sample were equidimensional with a diameter of ~10 μm. The chemical compositions of olivine grains were determined using a JEOL JXA8900R electron microprobe (EPMA) (Table 1). No chemical zoning was detected across the grains. These results indicate chemical equilibrium was reached during the one-atmos- phere annealing step. Electron transparent specimens were prepared for TEM analysis by ion-milling with 3 keV Ar^+ ions at low angle of 4–15° to minimize selective thinning along grain boundaries during milling.

RESULTS

Elemental segregation determined from STEM/EDX profiles across grain boundaries in the three different specimens is shown in Figure 1. All the analyzed boundaries are high-angle (>10°) grain boundaries as determined by electron diffraction patterns from both neighboring grains. The compositional fluctuations shown in Figure 1 are also present in the profiles of raw X-ray counts and do not result as an artifact of the conversion of X-ray counts to concentrations, which imposes the constraint that the concentrations sum to unity. Multiple samples and two or more boundaries per specimen were examined to confirm that the profiles shown in Figure 1 are representative. The negative compositional values of trace elements with low concentrations in the olivine grains are indicative of the statis-

TABLE 1. Olivine compositions (in wt%)

olivine	MgO	SiO_2	FeO	CaO	TiO_2	Al_2O_3	NiO	MnO	Total
Ivrea	49.23	40.42	9.91	0.03	–	–	0.40	0.15	100.14
Kilauea, Hawaii	48.07	40.29	11.38	0.31	0.04	0.08	0.38	0.16	100.70
Synthesized olivine + diopside	49.36	41.66	8.85	0.43	0.01	–	0.37	0.13	100.81

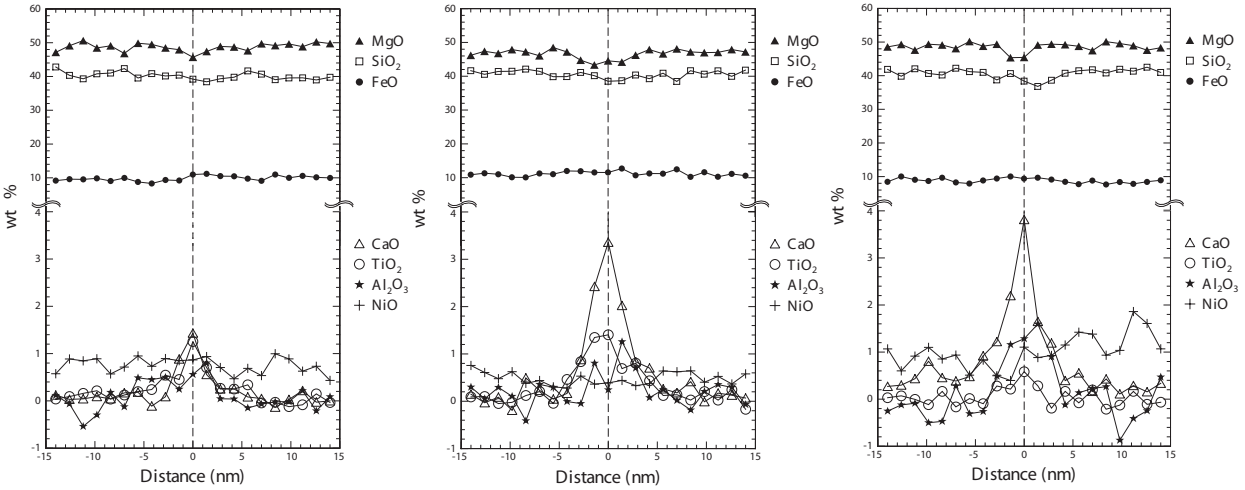

FIGURE 1. Chemical composition vs. distance from grain boundary based on STEM/EDX analyses of samples from (**a**) Ivrea Zone, (**b**) Kilauea, Hawaii, and (**c**) synthetic olivine + diopside aggregate. The precision of the measured compositions is evident from the statistical scatter of the data.

tical scatter in the spectral fitting procedure, as discussed previously.

A number of features can be identified as common to the three profiles. The width of the zone of segregation at each grain boundary is ~5 nm. Also, for all three samples, we detected: (1) no measurable partitioning of the major components FeO and SiO_2 or the minor component NiO; (2) mild depletion of the major component MgO; and (3) enrichment of the minor components CaO, TiO_2, and Al_2O_3 at the grain boundary. The degree of CaO enrichment is greater than that of TiO_2 or Al_2O_3 and varies among the specimens. The level of Al enrichment at grain boundaries is difficult to quantify because its spectral lines lie between those of Mg and Si, major elements in the olivine grains with count rates two orders of magnitude higher than that of Al; however, qualitatively its enrichment is clear.

Trace-element segregation to the boundaries of the Kilauea sample, characterized by summing many profiles acquired from the same grain boundary to obtain measurable intensities, is shown in Figure 2. The spatial resolution is somewhat degraded because some profiles were acquired from thicker parts of the specimen, and/or from parts where the grain boundary plane was tilted with respect to the incident electron beam in order to achieve the requisite signal. Chromium segregation is clear whereas no Mn segregation is apparent. Although the signal level for Sr achieves a maximum at the boundary position in Figure 2, the signal-to-noise ratio is insufficient to identify whether segregation is present or absent.

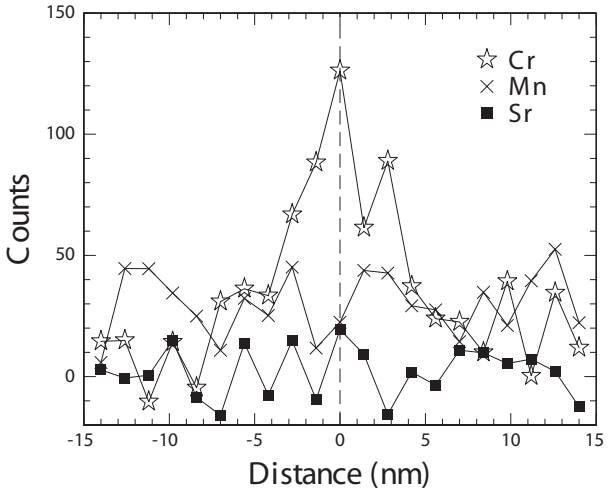

FIGURE 2. X-ray intensity profile from STEM/EDX analysis for trace elements in the vicinity of the grain boundaries in Kilauea, Hawaii sample.

DISCUSSION

We must consider the possible effect of grain boundary grooving (i.e., preferential ion-thinning at the boundary during TEM specimen preparation) on the composition profiles. Specimen thickness affects the total X-ray counts acquired at a given incident beam intensity. The approximately constant intensities of three major elements (Si, Fe, and O) across the boundary, to within the precision of the measurement, suggest that grain boundary grooving has had a negligible effect on the profiles. The amount of depletion and enrichment of Ca and Mg at grain boundaries are similar, suggesting that Ca substitutes for Mg at the boundaries.

The characteristic 5 nm width of the profiles in Figure 1 is not indicative of the width of the zone of segregation. In the regime of sample thickness necessary to acquire sufficient signal, this characteristic width is indicative of the scattering of the incident electrons in the specimen (i.e., beam broadening). The measured width of ~5 nm for the profiles therefore provides an upper bound on the true chemical width of the boundary, which is likely much narrower; the segregated elements could be confined entirely to the grain boundary plane, for example. Grain boundary segregation of Ca within a single atomic

plane has been observed in Ca-doped MgO (Yan et al. 1998). Similarly, the elemental concentrations at the grain boundary plane ($x = 0$) of the profiles provide a lower bound for the actual grain boundary composition.

A measure of the grain boundary segregation that is independent of either the spatial resolution of the measurement or the actual distribution of solute in the profile is the concentration of the solute per unit area of grain boundary integrated through the profile, which can be expressed either as atoms/cm^2 or effective monolayers. The latter measure provides an upper bound for the grain boundary concentration, as it represents the concentration if the solute were confined entirely to the grain boundary plane. The grain boundary coverage of Ca was calculated for the three specimens. Because the profiles indicate the substitution of Ca for Mg at the boundary, the coverage in monolayers assumes that Ca can occupy only the octahedrally coordinated regular lattice sites, M (M1 and M2). The volume concentration of these sites varies slightly with composition but is approximately $N_M = 2.69 \times 10^{22}$/cm^3. The areal concentration of such sites at the boundary is correspondingly $(N_M)^{2/3} = 8.98 \times 10^{14}$/cm^2; this area coverage corresponds to one monolayer of Ca at the boundary. The procedure for this calculation is analogous to that of Ikeda et al. (1993): the total excess Ca at the boundary is calculated with the greatest available statistical precision by taking the difference between boundary and matrix of all counts (both peak and background) within a energy window spanning the Ca*K* peaks in the X-ray spectrum; this excess Ca*K* intensity is converted to an atomic fraction using the electron microprobe concentration of Mg in the grain and the average count rate for Mg*K*α in the matrix; the atomic fraction is then converted to an grain boundary coverage using the density of octahedral M sites. The level of Ca grain boundary segregation in the three specimens is shown in Table 2. For all samples, note that the Ca coverage is well within one monolayer, indicating that all of the Ca could be accommodated at the grain boundary plane in all three specimens.

Enhancement of CaO, Al_2O_3, and TiO_2 at the contact between neighboring olivine grains has been previously reported. Suzuki (1987) measured CaO concentrations between grains of ~0.16 wt% with EPMA. This reported value actually corresponds to a level considerably in excess of those measured in the present study, because in Suzuki's study, the probe size was 2–3 μm, three orders of magnitude larger than that used in the present study. In fact, this level of segregation is greater than that produced by a 5 nm-thick film of pure CaO at the boundary and so is clearly inconsistent with the present study. In a TEM study, Wirth (1996) found thin (1–2 nm) amorphous films enriched in these same elements between neighboring olivine grains. He argued that the film was derived from grain boundary melting. In contrast, using high-resolution TEM imaging with resolution of better than 0.5 nm, Hiraga et al. (2002) determined that olivine grains are not separated by any secondary phase material even in partially molten synthetic peridotites. The observed segregation behavior was the same as that reported in this study. In contrast to the present and previous studies by Hiraga, the studies of both Suzuki and Wirth used mantle xenoliths from San Carlos, which—like most mantle xenoliths—have open or glass-lined boundaries. It is very likely that the process responsible for enrichment of specific elements between neighboring grains observed previously is different from that described here.

Other studies have reported solute enrichment along olivine grain boundaries similar to that observed in the present study, although some authors have concluded that the enrichment is due to the existence of thin melt films with thicknesses of ~1 nm (Drury and Fitz Gerald 1996; De Kloe et al. 2000; Tan et al. 2001). However, we have recently refuted the existence of thin films in partially molten peridotites (Hiraga et al. 2002).

The samples analyzed in the present study were formed in a variety of chemical environments and over a range of cooling rates. Under some circumstances, segregation in polycrystalline materials can be attributed to quenching, associated with diffusion of elements from the grain interior driven by a decrease in their solid solubility with decreasing temperature. Cooling times for natural samples are much longer than for laboratory specimens, possibly allowing some elements to diffuse into and/or out from the boundaries. However, because we observed significant segregation in water-quench samples, segregation must occur at elevated temperature indicating that it is an energetically favorable rather than simply a kinetically derived phenomenon for olivine-rich rocks.

Two driving forces are often considered in analysis of chemical segregation (e.g., Kingery 1974). First, strain energy minimization can explain the segregation of elements such as Ca, which have a much larger ionic radius than that of any of the cations in olivine. Such elements are likely to be accommodated with far lower strain energy at grain boundaries. Second, differences in the formation energy for cation and anion vacancies can cause segregation due to a build up of space charge at grain boundaries. To compensate for this space charge, heterovalent impurities such as Al substituting for Si can segregate to the grain boundaries. Hiraga et al. (in preparation) identified a positive correlation between the measured Ca concentration at olivine grain boundaries and that in the adjacent grains, indicating that grain boundary segregation is described by a partition coefficient. Such partitioning arises due to thermodynamic rather than kinetic factors, suggesting that segregation to grain boundaries is likely to occur deep in the Earth's mantle.

Clearly, grain boundaries can act as storage sites for the trace elements with very limited solubilities in olivine (Figs. 1 and 2). As discussed above, strain energy and space charge can

TABLE 2. Ca coverage at olivine grain boundaries

Specimen	Ivrea	Kilauea, Hawaii	Synthesized olivine + diopside
$\times 10^{14}$/cm^2	1.94 ± 0.31	6.07 ± 0.38	5.87 ± 0.43
monolayers*	0.216 ± 0.035	0.676 ± 0.042	0.654 ± 0.048

*Assumes Ca exclusively occupies octahedrally coordinated M sites.

drive segregation of elements to grain boundaries. Therefore, an element with a significantly different ionic radius and/or valence (e.g., a large-ion-lithophile or a high-field-strength element) than the element it replaces in the grain can be highly concentrated at grain boundaries; the concentrations and pattern of such elements are commonly used to infer the tectonic setting (e.g., Thompson et al. 1984). Segregation behavior similar to that observed in this study also occurs in partially molten ultramafic rocks (Hiraga et al. 2002). Thus, Ca, Al, and Ti must segregate to grain boundaries even in the presence of a phase (e.g., melt) that has a high solubility for these elements. Therefore, even if melt is completely extracted from mantle rocks under conditions of chemical equilibrium, these elements will still be present at grain boundaries. The observed segregation in the natural samples supports this hypothesis. In contrast, if a melt migrates quickly enough through a rock so as not to reach chemical equilibrium with the grains, it may still selectively dissolve elements stored at grain boundaries; the melt thus can become enriched in the elements concentrated at grain boundaries such as Ca, Al, Ti, and Cr. Formation of metasomatic mineral assemblages, reflecting the involvement of a Ca- and/or Ti-enriched melt (e.g., carbonatite) in mantle peridotite, might be explained by this process (e.g., Grégoire et al. 2000).

Grain boundary diffusion, which is often important during both deformation of rocks and chemical reactions to form new grains, is very sensitive to chemical segregation (e.g., Wuensch and Vasilos 1966). It is well known that impurities can slow grain boundary migration, a process described as "solute-drag." The observed segregation can hence influence the grain size of the rocks. In addition, segregation changes the structure of the grain boundary and thereby the grain boundary energy, which is an important driving force for grain growth. The influence of grain boundary segregation on these basic processes that determine the rheological behavior of rocks suggests that grain boundary segregation will influence the kinetics of dynamic processes in the Earth's mantle.

ACKNOWLEDGMENTS

M. Obata kindly provided the Ivrea rock sample. M.E. Zimmerman, Z. Wang, S. Majumder, and J. Hustoft kindly helped synthesizing aggregates. S-I Karato helped to select the natural samples. N. Abe gave us beneficial information of metasomatized mantle rocks. T.H. was funded by a JSPS Postdoctoral Fellowship for Research Abroad and a JSPS Research Fellowship for Young Scientists. This study was also supported by NSF through grants EAR-0079827 (MRI grant), EAR-0126277 and EAR-0106981. Research at the Oak Ridge National Laboratory SHaRE Collaborative Research Center was sponsored by the Division of Materials Sciences and Engineering, U.S. Department of Energy, under contract DE-AC05-00OR22725 with UT-Battelle, LLC. Critical reviews by K. Suzuki and an anonymous referee improved this manuscript.

REFERENCES CITED

Cooper, R.F. (1990) Differential stress-induced melt migration: an experimental approach. Journal of Geophysical Research, 95, 6979–6992.

De Kloe, R., Drury, M.R., and van Roermund, H.L.M. (2000) Evidence for stable grain boundary melt-films in experimentally deformed olivine-orthopyroxene rocks. Physics and Chemistry of Minerals, 27, 480–494.

Drury, M.R. and Fitz Gearld, J.D. (1996) Grain boundary melt films in an experimentally deformed olivine-orthopyroxene rock: implications for melt distribution in upper mantle. Geophysical Research Letters, 23, 701–704.

Fiori, C.E., Swyt, C.R., and Myklebust, R.L. (1992) Desktop Spectrum Analyzer and X-ray Database (DTSA) http://www.cstl.nist.gov/div837/Division/outputs/DTSA/DTSA.htm

Fraser, D.G., Watt, F., Grime , G.W., and Takacs, J. (1984) Direct determination of strontium enrichment on grain boundaries in a garnet lherzolite xenolith by proton microprobe analysis. Nature, 312, 352–354.

Grégoire, M., Lorand, J.P., O'Reilly, S.Y., and Cottin, J.Y. (2000) Armalcolite-bearing, Ti-rich metasomatic assemblages in harzburgitic xenoliths from the Kerguelen Island: Implications for the oceanic mantle budget of high-field strength elements. Geochimica et Cosmochimica Acta, 64, 673–694.

Gribb, T.T. and Cooper, R.F. (1998) Low-frequency shear attenuation in polycrystalline olivine: Grain boundary diffusion and the physical significance of the Andrade model for viscoelastic rheology. Journal of Geophysical Research, 103, 27,267–27,279.

Harris, D.M. and Anderson, A.T. (1983) Concentrations, sources, and losses of H_2O, CO_2, and S in Kilauean basalt. Geochimica et Cosmochimica Acta, 47, 1139–1150.

Hiraga, T., Anderson, I.M., Zimmerman, M.E., Mei, S., and Kohlstedt, D.L. (2002) Structure and chemistry of grain boundaries in deformed, olivine + basalt and partially molten lherzolite aggregates: Evidence of melt-free grain boundaries. Contributions to Mineralogy and Petrology, 144, 163–175.

Ikeda, J.A.S., Chiang, Y.-M., Garratt-Reed, A.J., and Vander Sande, J.B. (1993) Space charge segregation at grain boundaries in titanium dioxide: II, Model Experiments. Journal of the American Ceramic Society, 76, 2447–2459.

Jin, D., Karato, S., and Obata, M. (1998) Mechanisms of shear localization in the continental lithosphere: inference from the deformation microstructures of peridotites from the Ivrea zone, northwestern Italy. Journal of Structural Geology, 20, 195–209.

Kingery, W.D. (1974) Plausible concepts necessary and sufficient for interpretation of ceramic grain-boundary phenomena, II. Solute segregation, grain-boundary diffusion, and general discussion. Journal of The American Ceramic Society, 57, 74–83.

Obata, M. and Karato, S-I. (1995) Ultramafic pseudotachylite from the Balmuccia peridotite, Ivrea-Verbano zone, northern Italy. Tectonophysics, 242, 313–328.

Schwindinger, K.R. and Anderson, A.T. (1989) Synneusis of Kilauea Iki olivines. Contributions to Mineralogy and Petrology, 103, 187–198.

Shervais, J. (1979) Thermal emplacement model for the alpine lherzolite massif at Balmuccia (Italy). Journal of Petrology, 20, 795–820.

Suzuki, K. (1987) Grain-boundary enrichment of incompatible elements in some mantle peridotites. Chemical Geology, 63, 319–334.

Tan, B.H., Jackson, I., and Fitz Gerald J.D. (2001) High-temperature viscoelasticity of fine-grained polycrystalline olivine. Physics and Chemistry of Minerals, 28, 641–664.

Thompson, R.N., Morrison, M.A., Hendry, G.L., and Parry, S.J. (1984) An assessment of the relative roles of crust and mantle in magma genesis: an elemental approach. Philosophical Transactions of the Royal Society of London A, 310, 549–590.

Wirth, R. (1996) Thin amorphous films (1–2 nm) at olivine grain boundaries in mantle xenoliths from San Carlos, Arizona. Contributions to Mineralogy and Petrology, 124, 44–54.

Wuensch, B.J and Vasilos, T. (1966) Origin of grain-boundary diffusion in MgO. Journal of The American Ceramic Society, 49, 433–436.

Yan, Y., Chisholm, M.F., Duscher, G., and Pennycook, S.J. (1998) Atomic structure of a Ca-doped [001] tilt grain boundary in MgO. Journal of Electron Microscopy, 47, 115–120.

MANUSCRIPT RECEIVED OCTOBER 15, 2002
MANUSCRIPT ACCEPTED FEBRUARY 22, 2003
MANUSCRIPT HANDLED BY THOMAS DUFFY